RESEARCH ARTICLE

Key Points:
- Mesospheric temperatures from decay time of meteor radar have been estimated over low-latitude sectors in the Southern Hemisphere
- A good agreement between temperatures estimated by pressure method and from SABER data has been found
- The behavior of SAO on temperatures from meteor radars suggests an association with SAO on MLT zonal winds and diurnal tidal amplitudes

Correspondence to:
L. M. Lima,
lourivaldo_mota@yahoo.com.br

Meteor Radar Temperatures Over the Brazilian Low-Latitude Sectors

L. M. Lima[1] (iD), **P. P. Batista[2]** (iD), and **A. R. Paulino[1]** (iD)

[1]Departamento de Física, Universidade Estadual da Paraíba, Campina Grande, Brazil, [2]Divisão de Aeronomia, Instituto Nacional de Pesquisas Espaciais, São José dos Campos, Brazil

Abstract Meteor radar observations have been used to estimate the mesospheric temperatures at 90-km height over the Brazilian low-latitude sectors by applying gradient- and pressure-based techniques. The measurements have been taken from meteor radars operating at Cachoeira Paulista (22.7°S, 45°W), from 2002 to 2006, and São João do Cariri (7.4°S, 36.5°W), between mid-2004 and 2008. The temperatures estimated from meteor data by the two techniques, using local models for temperature gradient and pressure, showed a good agreement with temperatures from Sounding of the Atmosphere by Broadband Emission Radiometry over both sites. The seasonal behavior of the temperatures estimated from meteor data, and from Sounding of the Atmosphere by Broadband Emission Radiometry instrument, is characterized by a semiannual oscillation (SAO) with maximum values during equinoxes, which coincide with the westward phase of the mean zonal wind as well as with SAO on diurnal tidal amplitudes over both sites. The lag phases between SAO on temperatures and on winds (or on diurnal tidal amplitudes), near equator, have been stable in time indicating a seasonal cycle and the dynamic coupling of the tropical mesosphere through nonlinear interactions between oscillations from stratosphere. Although the time series used are short to establish reliable trends or solar effects, the temperatures over Cachoeira Paulista showed a decrease between 2003 and 2006, just when F10.7 index has declined in a rate of 15.3 sfu/year, while over São João do Cariri only a slight decay has been observed on temperatures by gradient technique obtained from mid-2004 to 2008, when F10.7 decrease rate was 9.2 sfu/year.

1. Introduction

The mesospheric temperature from meteor radar measurements has been estimated taking advantage of the fact that D_a is proportional to T^2/P, in which the ambipolar diffusion coefficient D_a can be derived from decay time of the radar signal and a suitable model to pressure P has been adopted, generally requiring calibration with temperatures obtained by other techniques (e.g., Dyrland et al., 2010; Hall et al., 2006; Holdsworth et al., 2006). An alternative method was developed by Hocking (1999), in which the absolute temperature is estimated using the slope of $\log_{10} D_a$ as a function of height. The method permits to determine the temperature without the knowledge of the pressure or of a pressure model; however, an appropriate model for the temperature gradient (dT/dz) is required.

After performing comparisons between Antarctic mesospheric temperatures estimated by these two techniques (pressure and temperature gradient methods), Holdsworth et al. (2006) have recommended the use of the pressure method, provided that a properly designed local pressure model be adopted. In this sense, a suitable pressure model has been used to estimation of temperatures from meteor data at high latitudes in the Northern Hemisphere. To obtain realistic variations of temperature from meteor measurements at 69°N and 78°N, Hall et al. (2006) have applied a calibration using pressure values from MSISE-90 data along with temperatures obtained by optical methods. Temperatures derived from measurements by sensors on board the satellites were used by Dyrland et al. (2010) to calibrate temperatures estimated from Svalbard (78°N) meteor radar measurements.

Kumar (2007) has used a combination of the temperature-pressure parameter relationship and the temperature from gradient technique to obtain the pressure at 90 km and, then, to remake the 82- to 98-km height profiles of pressure and temperature at Thumba (8.5°N). Their results were compared with temperature from Sounding of the Atmosphere by Broadband Emission Radiometry (SABER) instrument on board the Thermosphere Ionosphere Mesosphere Energetics and Dynamics (TIMED) satellite and showed reasonably good

agreement. Meek et al. (2013) have compared the meteor radar temperature by gradient and pressure methods at Eureka (80°N) with those available by the Earth Observing System Microwave Limb Sounder (MLS) on board the Aura satellite and have found that meteor radar temperature from both methods agrees quite well with MLS data for winter, but not during summer. The temperature gradient model was also applied to estimate the mesopause temperature from meteor radar data at Kunming (25.6°N), and the results were in good agreement with temperatures from SABER data (Yi et al., 2016).

The linear relationship between the width of meteor height distribution and the temperature measurements of the MLS on board the Aura satellite has been used by Lee et al. (2016) for estimating the temperature for meteor peak height at King Sejong Station, Antarctica (62°S). Liu et al. (2017) also used the width of meteor height distribution, but along with SABER temperature, for estimating the 90-km temperature at Mohe (53°N), China. In both studies the results have pointed out to a good performance in the temperatures obtained.

The mesopause temperature is characterized by a semiannual oscillation (SAO) in a global scale, which have been associated with the SAO in the zonal wind component, with maximums observed at the equator and at high latitudes and a minimum at middle latitudes. However, most of the studies on the temperature estimation from the measurements by meteor radars have used observations obtained in middle and high latitudes, and only a few analyzed low-latitude regions, which are generally located in the Northern Hemisphere. In this paper, we have used observations from meteor radars in the Southern Hemisphere, at Brazilian low-latitude sectors, to estimate the daily temperature near mesopause region and the results obtained by the use of gradient and pressure methods are compared with the temperature from SABER data. The temperatures obtained are then used in the analysis of SAO and its possible relationship with the SAO on zonal winds and on diurnal tidal amplitudes.

2. Observations

The mesopause temperatures evaluated are based on observations that have been taken from two meteor radars operating at low latitudes in the Southern Hemisphere; one of them is located at São João do Cariri (7.4°S, 36.5°W) and the other at Cachoeira Paulista (22.7°S, 45°W) in the Brazilian northeast and southeast regions, respectively, which already have been described (e.g., Araújo et al., 2014; Lima et al., 2012). Both systems are all-sky interferometric meteor radars with one 3-element transmitting and five 2-element receiving Yagi antennas, operating at a frequency of 35.24 MHz, with pulse width of 13.3 μs, repetition rate of 2144 Hz, and peak power of 12 kW. The data used in this work include meteor radar measurements at São João do Cariri, observed over the period July 2004 to December 2008, and at Cachoeira Paulista, obtained from January 2002 to July 2006.

The geometric height of each meteor trail is calculated from a combination of the meteor range and their direction of reflection point, which is computed from phase differences of the echoes' signals between the distinct receivers (Jones et al., 1998). In general, meteoroids ablate at heights between 140 and 70 km; however, due to the height ceiling effect, these very high frequency radars are able to detect meteor trails in the 110- to 70-km range.

Since the estimation of temperatures from meteor radar measurements is based on signal from underdense echoes, it is necessary to apply constraints to use the most representative data. In this sense, to estimate the daily temperatures, we have considered a 3-day window with a sufficient number of echoes (more than 2,000). The use of a 3-day window also reduces the tidal effects on daily temperatures. To remove outliers and biased values, we have considered the typical procedures applied by a number of authors (e.g., Hocking, 1999; Hocking et al., 1997; Holdsworth et al., 2006), such as removal of the data from echoes at the edges of the vertical meteor distribution (the upper and lower 5% of the meteors), as well as echoes at zenith angles greater than 60°. The data are also limited to echoes with signal-to-noise rate between 5 and 21 db to avoid contamination due to weaker and stronger meteor trails (Ballinger et al., 2008). It is observed that above 95 km the diffusion coefficients are lower than supposed and higher than expected below 85 km (Ballinger et al., 2008; Hall et al., 2005) causing a change in the gradient of $\log_{10} D_a$ around these heights (Younger et al., 2014). Therefore, we have considered the echoes observed between 85 and 95 km, since in this range the exponential growth of the ambipolar diffusion coefficient with height is practically fulfilled (Ballinger et al., 2008).

We also use daily mean temperatures obtained by SABER/TIMED instrument observations for comparisons. The SABER instrument is an infrared radiometer with 10 channels ranging from 1.27 to 16 μm. The instrument derives the vertical profiles of kinetic temperature from limb observations of CO_2 emissions with systematic
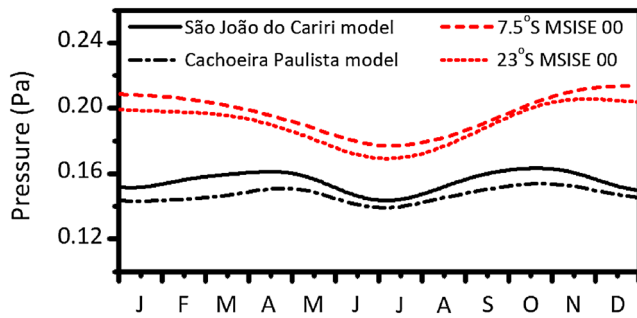
Figure 1. The local pressure models for São João do Cariri (black solid line) and Cachoeira Paulista (back dash-dotted line). Pressure from MSISE-00 parameters are represented for 7.5°S (red dashed line) and 23°S (red dotted line).

uncertainty of 4 K around 90 km (Remsberg et al., 2008). In this study, we used the level 2A kinetic temperature version 2.0 data and the daily mean temperature around 90 km was obtained from temperature profiles observed in a 10° × 10° grid centered on the radar locations. The SABER data observed from 2004 to 2008 were used to obtain daily temperatures over the São João do Cariri site, while the SABER data from 2002 to 2006 were considered to Cachoeira Paulista.

3. Method and Results

The dissipation of the meteor trail is mainly dominated by ambipolar diffusion and defines the intensity of the signal from underdense echoes, that is, from a trail that has an electron line density less than 10^{14} m^{-1} (McKinley, 1961). The signal amplitude of the underdense echoes exponentially decreases as a function of time, and half-life time, $\tau_{1/2}$, is defined as the time for the signal amplitude to drop to half the initial value, as follows:

$$\tau_{1/2} = \frac{\lambda^2 \ln 2}{16\pi^2 D_a} \tag{1}$$

in which λ is the wavelength correspondent to the radar frequency and D_a is the ambipolar diffusion coefficient.

To estimate the mesopause temperature from meteor data, Hocking et al. (1997) have used the Einstein relation for ambipolar diffusion coefficient, which has been discussed by Chilson et al. (1996) and is expressed as follows:

$$\frac{T^2}{P} = \frac{q_e}{2k}\left(\frac{273.16}{1.013 \times 10^5 K_0}\right)\left(\frac{\lambda^2 \ln 2}{16\pi^2 \tau_{1/2}}\right) \tag{2}$$

in which P is the neutral atmospheric pressure (Pa), q_e is the electron charge, k is the Boltzmann constant, and K_0 is the ion mobility in the meteor trail (= 2.5×10^{-4} m^2/s). As mentioned, to estimate the temperature using this pressure method, it is necessary to provide a local pressure model (Holdsworth et al., 2006).

In the absence of a suitable local pressure model for two sites, we have adopted pressure around 87 km inferred from the ambipolar diffusion coefficient and a temperature model based on the airglow OH rotational temperatures (Takahashi et al., 2004, 2005). The temperature models for the height of 87 km have been set up considering the seasonal behavior of the OH temperatures at Cachoeira Paulista and São João do Cariri (e.g., Buriti et al., 2001; Shepherd et al., 2004; Takahashi et al., 1995). The temperatures from the models along with the smoothed diffusion coefficient at 86–88 km were used to obtain the pressure for 87 km, by equation (2). The local pressure model at 90 km has been reached considering that $P_{90} = P_{87} \exp(-3/H)$, in which H is the scale height, which has been taken from the seasonal behavior of $S_m \times \log_{10}(e)$.

The local pressure models for São João do Cariri (black solid line) and Cachoeira Paulista (black dash-dotted line), as well as pressure model obtained from parameters of NRLMSISE-00 empirical Atmosphere Model (Picone et al., 2002), are represented in Figure 1 for 7.5°S (red dashed line) and 23°S (red dotted line).

Alternatively, Hocking (1999) has used the relationship between $\log_{10}(1/\tau_{1/2})$ and $\log_{10}(P)$ as well as the fact that variation of P with altitude depends on the scale height (H), to show that the slope (S_m) of the scatter plot of $\log_{10}(1/\tau_{1/2})$ versus height (z) is related to the mean temperature at the meteor peak height, leading to the following expression for temperature:

$$T = S_m\left(\frac{mg}{k} + 2\frac{dT}{dz}\right)\log_{10} e. \tag{3}$$

In this equation, g is acceleration due to gravity at 90 km (=9.5 ms^{-2}), m is the mass of an average air molecule (=4.749 ×10^{-26} kg), and the temperature gradient (dT/dz) was taken from a model based in Hocking et al. (2004). It should be noted that the temperature gradient model does not show significant seasonal variability for latitudes below 30°.

The temperatures estimated by gradient technique (black filled circle), using a 3-day radar data window, are shown in Figure 2 for Cachoeira Paulista's measurements (top panel) registered from January 2002 to July 2006
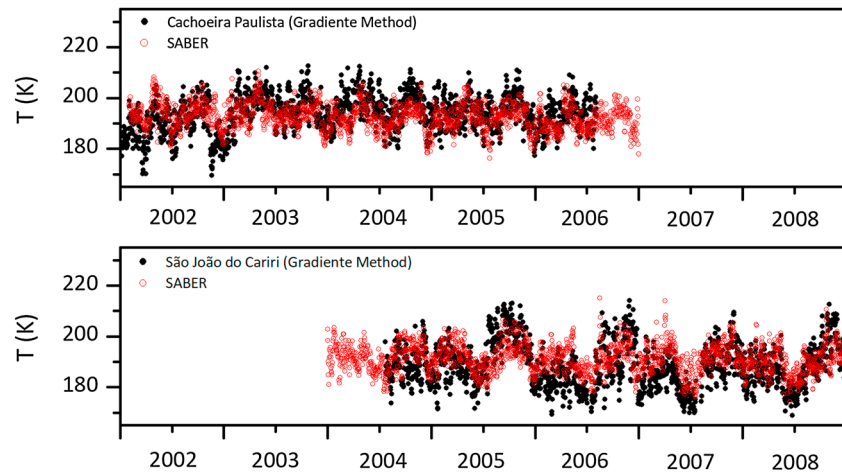
Figure 2. Mesopause temperature from gradient method (black filled circle) for Cachoeira Paulista (top panel) and São João do Cariri (bottom panel). Red open circle represent the SABER temperatures. SABER = Sounding of the Atmosphere by Broadband Emission Radiometry.

and for the observations at São João do Cariri (bottom panel), obtained from July 2004 to December 2008. The SABER temperatures are also represented by a red open circle. The higher temperatures estimated from Cachoeira Paulista meteor data exceed those from SABER instrument during 2003–2005, with the lowest values have been obtained in 2002. A moderated correlation between them has been found ($r = 0.38$). The temperatures estimated from São João do Cariri meteor data have shown a good concordance with SABER temperatures, but, as at Cachoeira Paulista, a wider scatter than the SABER temperatures can also be observed throughout all the years. The correlation between meteor radar and SABER temperatures at São João do Cariri was better than at Cachoeira Paulista, with $r = 0.48$. The larger day-to-day variation observed in the temperature obtained by gradient method has been discussed by Holdsworth et al. (2006). It should be remembered that a small day-to-day variation in slope results in large fluctuations in temperature, different from the methods that use local calibration with satellite measurements, such as the full width at half maximum method (Lee et al., 2016), that produces a smoothed day-by-day variation in the temperatures.
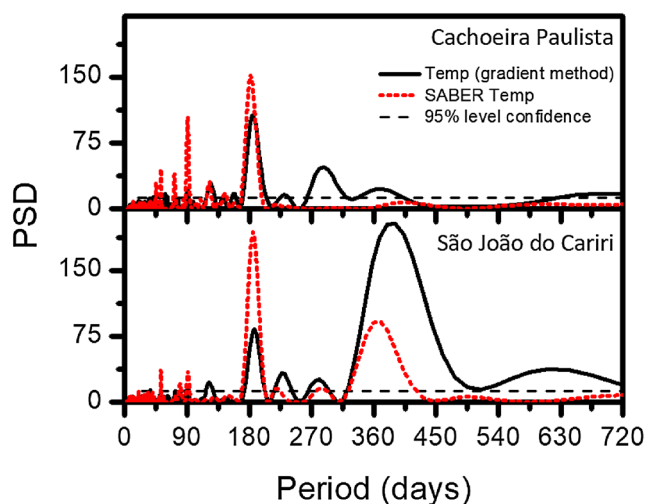

Figure 3. Lomb-Scargle periodograms for mesopause temperatures from gradient method (black line) and SABER (red dotted line) for São João do Cariri (bottom panel) and Cachoeira Paulista (top panel). Horizontal dash-dotted line represents the 95% confidence level. SABER = Sounding of the Atmosphere by Broadband Emission Radiometry. PSD = Power Spectral Density.

In order to identify seasonal periodicities, both time series (meteor radar and SABER temperatures) have been subjected to spectral analysis by Lomb-Scargle periodogram technique (Scargle, 1982) and the results showed in Figure 3 have revealed the presence of spectral energy associated with annual oscillation (AO) and SAO for meteor radar and SABER temperatures at two sites. A quarterannual oscillation (QAO) also is present at both sites; however, the spectral energy in the meteor radar temperatures is weaker than those from SABER instrument. Additional peaks for meteor radar temperature have been observed for periods of 287 days at Cachoeira Paulista and of 625 days at São João do Cariri, which are not seen in the respective SABER temperatures. On the other hand, SABER temperatures have shown peaks for periods near 90 days and below, which have not been captured by the temperatures obtained from radar measurements. These periodicities may be associated with intraseasonal oscillations, as well as due contamination by TIMED satellite yaws.

The seasonal behavior is better seen from the composite year, which is set up by superimposing the daily temperatures available on each site to produce their respective composite years. Figure 4 shows the composite year of the mesopause temperature from gradient method (black circle and dotted line) and their yearly standard deviation (gray), along with the harmonic fitting (red line) for São João do Cariri (bottom panel) and Cachoeira Paulista (top panel). The composite fit has been obtained by harmonic
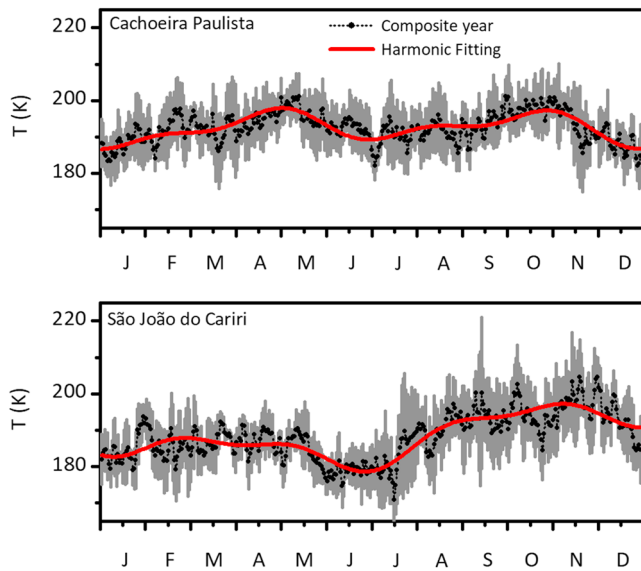
Figure 4. Composite year of the mesopause temperature from gradient method (black circle and dotted line) and scattering (gray) along with the harmonic fitting (red line) for São João do Cariri (bottom panel) and Cachoeira Paulista (top panel).

analysis considering that the deviations of the signals around the mean are due to the AO, SAO, and QAO for both sites.

As can be seen in Figure 4, the temperatures over both sites show a clear SAO with amplitude of 3.7 K for Cachoeira Paulista and 3.8 K for São João do Cariri, in which the maximum occurs during April–May and October–November (around equinoxes), and the minimum happens during December–February and June–July (around solstices). On São João do Cariri, SAO presents a marked asymmetry, in which temperatures for August–November are higher than those during February–May. The mean temperatures from composite years have been found to be of 192.5 K and 188.1 K for Cachoeira Paulista and São João do Cariri, respectively. The standard deviation (gray) indicates that meteor radar temperature obtained by gradient technique undergoes considerable variability from year to year. It is noted that, over São João do Cariri, variations in temperatures were higher in the second semester (winter and spring seasons), while the spread of the temperatures during summer and autumn seasons was smaller.

Figure 5 shows the daily temperatures estimated by pressure method (black filled circle) at Cachoeira Paulista (top panel) and at São João do Cariri (bottom panel), for the same periods considered in Figure 2. Once more, SABER temperatures are represented by a red open circle. The temperatures estimated from meteor data over Cachoeira Paulista are lower than those of the SABER instrument from mid-2004 to mid-2006; however, in general, there is a good concordance between temperatures by meteor pressure method and those from SABER data with a correlation of $r = 0.55$. A good concordance has also been found between temperatures by meteor pressure method and those from SABER measurements over São João do Cariri ($r = 0.58$).

The Lomb-Scargle periodogram results for temperatures by meteor pressure method are very similar to those obtained for SABER temperatures (red dotted line in Figure 3) and have shown the presence of a strong SAO. Moreover, the meteor temperatures over São João do Cariri also showed a peak in AO. As identified in the meteor temperatures obtained by gradient technique, a weak QAO periodicity is also present at both sites in meteor radar temperatures by pressure method.

The composite year of the temperatures obtained by pressure method is represented in Figure 6 (black dotted line) with their standard deviations (gray) for São João do Cariri (bottom panel) and Cachoeira Paulista (top panel). Again, the red lines represent AO, SAO, and QAO harmonic fitting for both sites. From this figure,
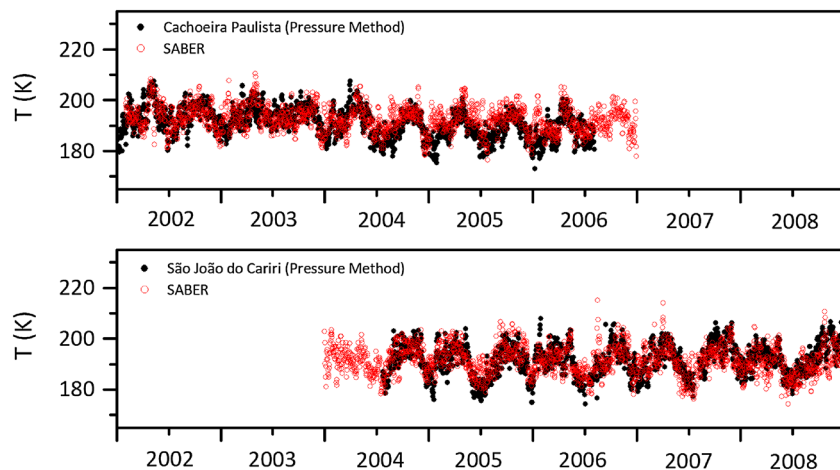

Figure 5. Mesopause temperature from pressure method (black filled circle) for São João do Cariri (bottom panel) and Cachoeira Paulista (top panel). Red open circle represent SABER temperatures. SABER = Sounding of the Atmosphere by Broadband Emission Radiometry.
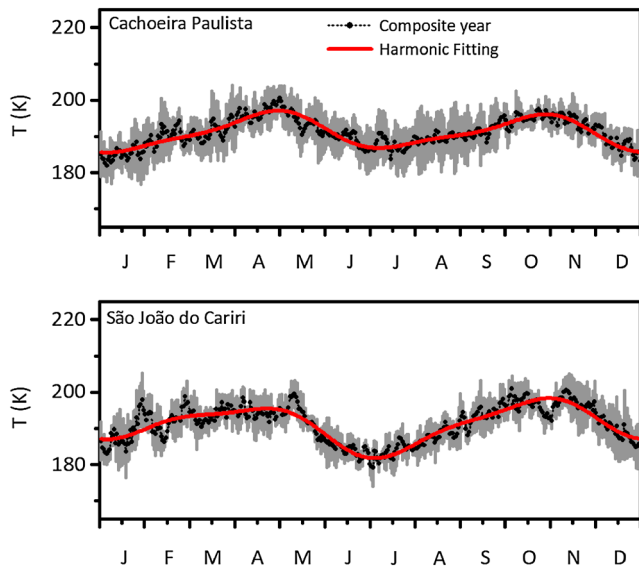
Figure 6. Composite year of the mesopause temperature from pressure method (black circle and dotted line) and dispersion (gray) along with harmonic fitting (red line) for São João do Cariri (bottom panel) and Cachoeira Paulista (top panel).

we have that temperature dispersions estimated by pressure method are lower than those observed for temperatures obtained by gradient technique (Figure 4). Year-to-year variability was higher during winter months (July–September) over Cachoeira Paulista; however, over São João do Cariri this variability was lower just during winter time.

A mean temperature of 191 K have been obtained from composite year fitting for both sites, and, as in the case of temperatures estimated by gradient technique, the temperatures obtained by pressure method show a seasonal behavior characterized by the presence of strong SAO with amplitudes of 4.7 and 5.6 K for Cachoeira Paulista and São João do Cariri, respectively. The occurrences of the maximums are coincident for temperatures estimated by both methods, that is, maximums around equinoxes and minimums around solstices. Looking at Figures 4 and 6, it is verified that the behavior of the meteor temperatures over São João do Cariri, by pressure method, does not show the pronounced asymmetry observed for temperatures by gradient technique.

To examine the interannual variability on temperatures, 45-point smoothed data series have been obtained from each daily sequence of the temperature estimated by both techniques and from SABER data. In Figure 7 are shown the 45-point smoothed temperature estimated by gradient technique (black dash-dotted line), by pressure method (blue line) and from SABER data (red dotted line) for São João do Cariri (bottom panel) and Cachoeira Paulista (top panel).

From this figure, we can notice that the mesopause temperature estimated from meteor radar data by two techniques, as well as from SABER data, reveals interannual variability over both sites. In general, the temperature estimated by pressure method follows the interannual behavior of SABER temperature with some episodes of phase shift between them for both sites; however, a better agreement is observed between interannual behaviors of these temperatures on São João do Cariri. The temperature estimated by gradient technique over both sites exhibits strong interannual variability, which in turn presents episodes of disagreement with both SABER and pressure method temperatures.

It is still possible to notice that from 2002 to 2006, SABER temperatures on Cachoeira Paulista presented a slight decline, whereas for the temperatures estimated by pressure method this decline is more pronounced; however, this feature is not visualized in the temperatures estimated by gradient technique, neither in the temperatures estimated by both gradient and pressure techniques as well as from SABER data over São João do Cariri during the time interval from 2004 to 2008. To explore this feature, temperature residuals have been obtained. For this, the semiannual variation has been extracted from daily temperatures for each year and
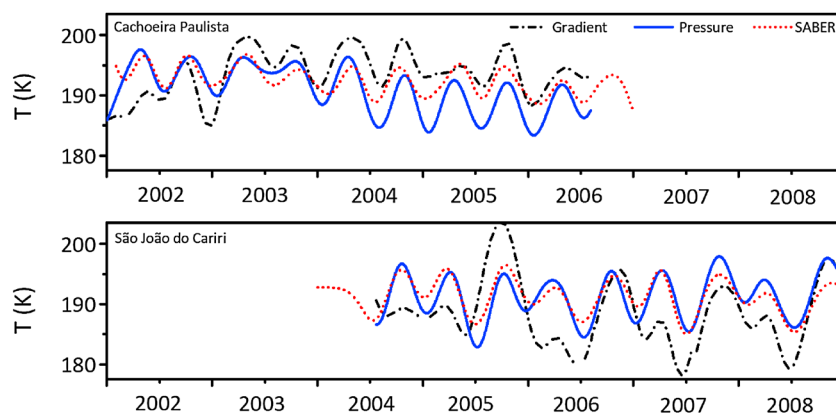

Figure 7. Smoothed temperatures estimated by gradient technique (black dash-dotted line), pressure method (blue line), and from SABER data (red dotted line) for São João do Cariri (bottom panel) and Cachoeira Paulista (top panel). SABER = Sounding of the Atmosphere by Broadband Emission Radiometry.
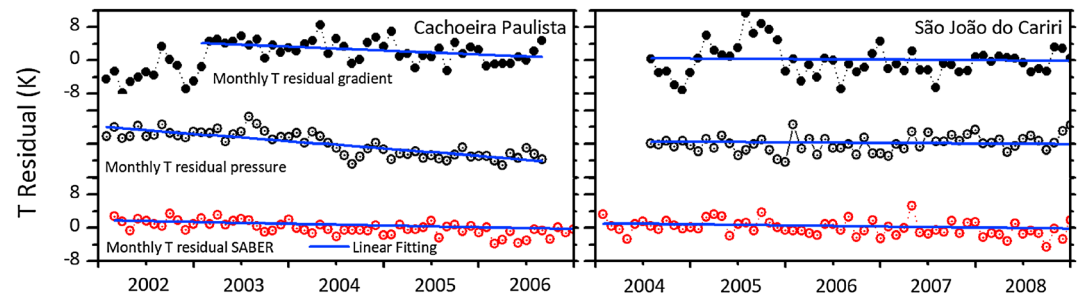
Figure 8. Monthly residuals of temperatures from gradient technique (black full circle), pressure method (black open circle), and from SABER data (red open circle) for Cachoeira Paulista (left) and São João do Cariri (right). Blue lines represent the linear trends. SABER = Sounding of the Atmosphere by Broadband Emission Radiometry.

monthly averages of the temperature residuals were then determined, once the SAO is the strongest among the others and their removal from the data were satisfactory to obtain the trend from the series of monthly averages. The monthly residuals are shown in Figure 8 for temperature from gradient technique (black full circle), pressure method (black open circle), and from SABER data (red open circle) along with their respective linear trends (blue line) for Cachoeira Paulista (left) and São João do Cariri (right).

From linear fitting, we have perceived that the temperature estimated by gradient technique over Cachoeira Paulista increases by 0.8 K/year from 2002 to 2006, but when we considered the time interval from 2003 to 2006, we found a decreasing rate of 0.9 K/year (represented by a blue line). The temperature estimated by pressure method shows a decay rate of 1.7 K/year, and from SABER data, a decay rate of 0.7 K/year has been obtained. From linear fitting for monthly residuals over São João do Cariri, we have found that the temperature estimated from 2004 to 2008, by gradient technique and from SABER data, decays by 0.3 and 0.4 K/year, respectively, but the temperature from pressure method increases by 0.4 K/year.

4. Discussion

The mesopause temperature estimated from meteor radar observations by gradient technique and pressure method shows good agreement with temperatures from SABER data over Cachoeira Paulista and São João do Cariri; however, the temperature obtained by gradient model presents larger day-to-day variations than those obtained by pressure model and from SABER instrument for both sites, confirming findings reported in previous studies (e.g., Holdsworth et al., 2006; Yi et al., 2016). The mesopause temperatures estimated by gradient and pressure techniques for both sites clearly reproduce a seasonal behavior characterized by SAO, which have also been observed in other studies for these latitudes (Buriti et al., 2001; Huang et al., 2006; Shepherd et al., 2004; Takahashi et al., 1995).

The amplitude of the SAO viewed on the composite year for the temperature estimated over Cachoeira Paulista by pressure method (4.7 ± 0.1 K) exceeds the SAO temperature's amplitude by gradient method (3.7 ± 0.2 K), which exceeds the SAO temperature's amplitude depicted on year's composite from SABER data (2.9 ± 0.2 K). Using nocturnal airglow OH rotational temperature obtained by photometer, Takahashi et al. (1995) have found SAO amplitude of 3.5 K for altitude around 87 km at Cachoeira Paulista, and Shepherd et al. (2004), using daily zonal mean temperature at 87-km height from Wind Imaging Interferometer, have found SAO amplitudes of 3.6 and 2.4 K for 20°S and 25°S, respectively. Using temperatures from SABER data, Huang et al. (2006) have estimated a SAO amplitude range of 2.5–3.0 K near 24°S around 90-km height.

The SAO amplitude obtained from the temperature's composite year by pressure method (5.5 ± 0.1 K) over São João do Cariri also exceeds those estimated from gradient technique (3.8 ± 0.2 K) and from SABER data (3.5±0.4 K). Buriti et al. (2001) have estimated a SAO amplitude of 6.8 K from nocturnal airglow OH temperature around 87-km height by photometer at São João do Cariri, while Shepherd et al. (2004) have obtained SAO amplitudes of 4.4 K for 5°S and 3.7 K at 10°S from Wind Imaging Interferometer temperature data around 87-km height. The SAO amplitude estimated from SABER temperature data by Huang et al. (2006) is in the 4.5- to 5.5-K range near 7°S around 90-km height.

It is believed that the driving mechanism of the mesospheric SAO in the zonal mean wind is the selective filtering of gravity and Kelvin waves by stratospheric SAO (Dunkerton, 1982; Sassi & Garcia, 1997) and that the
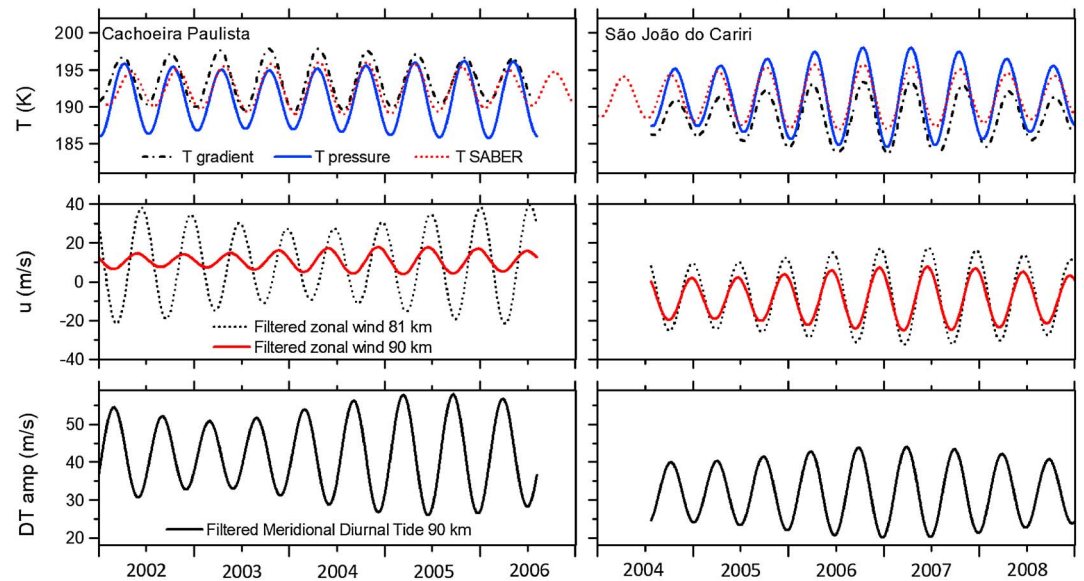
Figure 9. SAO on temperatures (top panels) estimated by gradient (black dash-dotted line) and pressure (blue line) techniques and by SABER (red dotted line) data, along with SAO on zonal winds (middle panels) at 81 km (black dotted line) and 90 km (red dotted line) and SAO on meridional diurnal tidal amplitudes (bottom panels) observed over Cachoeira Paulista (left column) and São João do Cariri (right column). Data have been band-pass filtered to retain periods between 172 and 192 days. SABER = Sounding of the Atmosphere by Broadband Emission Radiometry; SAO = semiannual oscillation; DT = diurnal tide.

mesospheric SAO in temperature is associated with them. However, the seasonal change in the atmospheric tidal amplitudes may also affect the temperature of mesospheric SAO. A look at local mesosphere/lower thermosphere (MLT) dynamics provides insights to understand such associations. The MLT zonal mean winds over Cachoeira Paulista are characterized by SAO below 90 km (Batista et al., 2004), while over São João do Cariri this variation appears in all MLT region, that is, in the 80- to 100-km range height (Lima et al., 2007). Diurnal tide amplitudes in the MLT winds over both sites exhibit a semiannual variation with strongest amplitude reaching maximum values during February–April and a second amplification occurring during August–October for both zonal and meridional components.

Figure 9 depicts the SAO's evolution over time on temperatures (top panels), on zonal winds (middle panels) at 81- and 90-km heights, and on amplitudes of the meridional diurnal tide (bottom panels) at 90-km height for Cachoeira Paulista (left column) and for São João do Cariri (right column). For obtaining the filtered data series, the daily temperature, zonal winds, and diurnal tidal amplitudes were subjected to a band-pass filter with cutoff periods of 172 and 192, days.

From Figure 9 it is possible to notice that SAOs on temperatures are in phase with each other (mainly for temperatures by pressure method and from SABER data at São João do Cariri), in which the temperatures maximize around equinoxes, just during the westward phase of the SAO on zonal winds at 81 and 90 km, which coincides with the maximums in the amplitude of SAO on diurnal tide, for both sites. However, the maximum in the SAO on westward winds at 81 km happens about 30 and 18–30 days before the maximum in the temperatures at 90 km over Cachoeira Paulista and São João do Cariri, respectively.

The SAO in the mesospheric temperatures, zonal winds, and meridional diurnal tidal amplitudes exhibits the same interannual variability for São João do Cariri; that is, changes in the amplitude of the mesospheric SAO in temperatures correspond to those in the zonal winds and in diurnal tide amplitudes, while for Cachoeira Paulista the interannual variability in the amplitudes of SAO on meteor temperatures also follows those observed on diurnal tidal amplitudes and zonal winds at 81 km, but not at 90 km. The behavior of SAO on meteor radar temperatures is consistent with mesospheric SAO variability revealed from satellite data at lower latitudes (Garcia et al., 1997; Shepherd et al., 2004). A look at Figure 9 points to an apparent association between SAO on temperatures and on zonal winds below 90 km. However, it is interesting to note that the amplitudes of the SAO on zonal winds at 81 km exceed in 3 times those at 90 km over Cachoeira Paulista, while over São João do Cariri such amplitudes decrease more slowly with height. In its turn, the amplitude of SAO
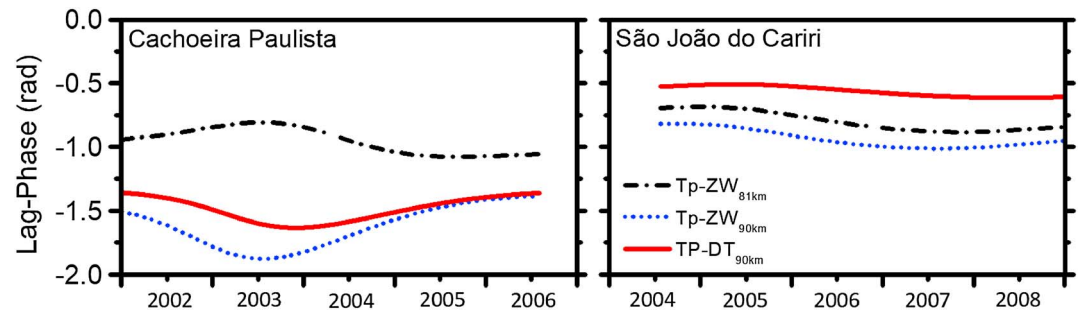
Figure 10. Lag phases for SAO coupling on temperature-zonal winds at 81 km (black dash-dotted line) and 90 km (blue dotted line) and for SAO coupling on temperature-diurnal tidal amplitudes (red line) observed over Cachoeira Paulista (left) and São João do Cariri (right) SAO = semiannual oscillation.

on meridional diurnal tide over Cachoeira Paulista surpasses around 4 m/s those of São João do Cariri, while the amplitude of SAO on temperature over São João do Cariri is slightly higher than the one over Cachoeira Paulista, in accordance with the classical tidal theory and observations. It is worth it remembering that diurnal tides in MLT winds maximize at low latitudes (20°), while diurnal tides in temperature maximize around the equator.

Consequently, the seasonal variation in diurnal tidal amplitude should also contribute to the SAO on temperature, since its break above 85 km contributes to change the mesospheric temperature. To see a possible coupling between SAO on temperature, zonal wind, and diurnal tide, the temporal evolution of the phase difference for temperature-wind and temperature-diurnal tidal SAO sets have been obtained by wavelet cross spectrum, and the results for SAO on temperature by pressure method are shown in Figure 10 (temperatures by gradient method and from SABER are similar). From the figure, we verify that SAO couplings at Cachoeira Paulista happen after those at São João do Cariri. The results have also revealed that, for Cachoeira Paulista, the SAO coupling for temperature-diurnal tidal at 90 km takes place quasi-simultaneously with the SAO coupling temperature-wind at 90 km, and both lag phase varied throughout the time. However, for São João do Cariri, the SAO coupling for temperature-diurnal tidal at 90 km happens before the SAO coupling for temperature-wind at 81 and 90 km, and all lag phases have been constant over time, indicating that SAO couplings over São João do Cariri apparently are in a phase-coherent state, which suggests a link between the seasonal cycle and the dynamics of the tropical mesosphere through the nonlinear interactions between oscillations from stratosphere. For example, the interannual variations observed in the mesospheric SAO on temperatures, zonal winds, and diurnal tidal amplitudes can be associated with the phase of quasi-biennial oscillation (QBO). Observational studies have pointed out a possible link between the phase of QBO and the interannual variations in the mesospheric SAO (deWit et al., 2013). On the other hand, Peña-Ortiz et al. (2010), using simulations, have suggested that inertia gravity waves and small gravity waves act as a force on the link between the QBO and the mesospheric SAO. Simulations by Gattinger et al. (2013) pointed out that interactions between vertical eddy diffusion and background vertical advection are involved in the generation of mesospheric SAO.

Although the temperature estimated from meteor radar measurements by both techniques presents good agreement as well as reproduces the already known seasonal variations, some differences in SAO amplitudes are evident. To better understand the role played in SAO amplitudes by local models adopted, we have analyzed equations (2) and (3), considering the local models of temperature gradient and pressure. If we adopt a constant pressure over time in equation (2), and an isothermal mesopause (i.e., $dT/dz = 0$) in equation (3), the SAO amplitude in temperature estimated by gradient technique (5.5 ± 0.2 and 3.8 ± 0.2 K) will exceed those obtained by pressure method (1.2 ± 0.1 and 1.0 ± 0.1 K, for Cachoeira Paulista and São João do Cariri, respectively). Therefore, it is verified that the seasonal behavior of the adopted temperature gradient favors the subtraction of SAO amplitude in temperature by gradient technique, mainly at Cachoeira Paulista, while the seasonal behavior of pressure favors the amplification of SAO in temperature by pressure model, which has possibly contributed for introducing uncertainty to the temperatures estimated by both techniques. It should be remembered that only the seasonal variation in local models of temperature gradient and pressure over the course of a year were considered, but these quantities are also subject to short term as well as interannual variations.

Investigations about long-term response to anthropogenic effects on MLT region have pointed out that an increase in greenhouse gases CO_2 and CH_4 have a consequent cooling of the stratosphere and mesosphere regions (Roble & Dickinson, 1989). Observational studies have reported trends and solar effects on temperatures around 87- and 90-km height from OH imager data, meteor echo fading times, and Lidar measurements at middle and high latitudes in the Northern Hemisphere (e.g., Hall et al., 2012; Offermann et al., 2010; She et al., 2015). The temperatures estimated by both techniques and from SABER data over Cachoeira Paulista have revealed a decrease over time (Figures 7 and 8), mainly between 2003 and 2006, only during the declining phase of the solar cycle 23, in which the monthly F10.7 solar radio flux index has experienced a drop rate of 15.3 sfu/year (1 sfu = 10^{-22} W·m^{-2}·Hz^{-1}). It is noteworthy that Lima et al. (2015) have found a relationship between decrease in meteor echo peak height over Cachoeira Paulista and the 11-year solar cycle. Over São João do Cariri, only a slight decay has been observed on temperatures estimated between mid-2004 and 2008 by gradient technique and from SABER data when the monthly F10.7 solar radio flux index declined in a rate of 9.2 sfu/year.

Despite the short period of data considered here, the results for Cachoeira Paulista are qualitatively consistent with those of Huang et al. (2016) that, using data from SABER instrument obtained between 2002 and 2014, have found a positive temperature response at 80- to 100-km height to solar variability for 48°N to 48°S latitude range, but the period of 13 years is not long enough to establish reliable trends. Venturini et al. (2018) have used SABER temperature to investigate MLT temperature variability and its trend in Brazilian southern (29.7°S) and founded a positive trend of 0.58 K per decade at 85 km, a negative trend of 0.02 K per decade at 90 km, and another positive trend of 0.41 K per decade at 95 km, from 2003 to 2014 (12 years), concluding that there is no variability tendency in MLT temperature. The authors also have noted that during years of maximum solar the temperature's amplitude is twice the amplitude of the year of solar minimum, deducing that amplitudes of annual and semiannual variation are directly influenced by the solar cycle. Analyzing Figure 9, we can perceive, from the evolution of the short time series, that the amplitudes of SAO on MLT temperatures over Cachoeira Paulista and São João do Cariri do not show direct modulation by the solar cycle. Araújo et al. (2017) did not find signals of solar cycle effects in the interannual variability of diurnal tidal amplitude over Cachoeira Paulista; instead, the QBO modulation of diurnal tide amplitude showed a quasi-decadal variation, in which the diurnal tidal amplitude modulation by QBO is stronger during years of maximum solar. Considering that the seasonal variation in diurnal tidal amplitude contributes to SAO on temperature and that there is a link between the phase of QBO and the interannual variations in the mesospheric SAO, then the QBO seems to play a key role in modulating the dynamic processes of the MLT region.

5. Summary

In this paper, we have estimated the daily temperatures at 90-km height from decay time of meteor radar signals over Cachoeira Paulista and São João do Cariri, Brazil, using gradient and pressure techniques. For this a local temperature gradient model based on Hocking et al. (2004), as well as a pressure model for 90-km height based on ambipolar diffusion coefficient and airglow OH temperature, has been set up. The results showed a good agreement with temperature measurements from SABER data, mainly those estimated by pressure method.

Spectral analysis has revealed the presence of AO, SAO, and QAO periods on temperatures estimated from meteor radar measurements by two techniques and from SABER data at both sites. The amplitude of the SAO over Cachoeira Paulista on temperatures estimated by pressure method exceeds those estimated by gradient technique, as well as SABER temperatures. Over São João do Cariri, the SAO amplitude on temperature estimated by pressure method also exceeds those derived by gradient technique and from SABER data. SAO temperatures are in phase with each other, with maximums around equinoxes, when the phase of SAO on mean zonal winds around 81 and 90 km is westward as well as with the maximums on meridional diurnal tidal amplitudes over both sites; however, the maximums in SAO on westward winds and on diurnal tidal amplitudes happen before the maximum in SAO on temperatures. The amplitude of the mesospheric SAO on temperatures, on zonal winds, and diurnal tidal amplitudes have shown similar interannual variations, mainly at São João do Cariri.

An interesting aspect that can be seen from lag phases between SAO on temperature and on winds and on diurnal tidal amplitudes is that at 7.4°S the SAO couplings are in a phase-coherent state, indicating a link between the seasonal cycle and the dynamics of tropical mesosphere through the nonlinear interactions

between oscillations from stratosphere. For 23°S, SAO couplings take place after those at 7.4°S and the lag phases varied throughout the time, which is not compatible with SAO couplings via nonlinear interactions.

A decrease on temperatures estimated by two methods over Cachoeira Paulista have been observed from 2003 to 2006, during the declining phase of the solar cycle 23, when the F10.7 index dropped by 15.3 sfu/year; while over São João do Cariri a slight decay on temperatures estimated by gradient technique from mid-2004 to 2008, when the F10.7 decreased by 9.2 sfu/year, has been revealed, but the data series used here are too short and, therefore, are not enough to derive neither long-term trends nor effects of the 11-year solar cycle on the temporal behavior of the estimated temperatures over the two sites.

Only the seasonal variation in the local models of the temperature gradient and pressure has been considered here, and therefore, it is necessary to undertake additional efforts in the improvement of these models, since they have possibly contributed to introduce uncertainties in temperature estimation from meteor radar measurements.

References

Araújo, L. R., Lima, L. M., Batista, P. P., Clemesha, B. R., & Takahashi, H. (2014). Planetary wave seasonality from meteor wind measurements at 7.4°S and 22.7°S. *Annales de Geophysique*, *32*, 519–531. https://doi.org/10.5194/angeo-32-519-2014

Araújo, L. R., Lima, L. M., Jacobi, C., & Batista, P. P. (2017). Quasi-biennial oscillation signatures in the diurnal tidal winds over Cachoeira Paulista Brazil. *Journal of Atmospheric and Solar - Terrestrial Physics*, *155*, 71–78. https://doi.org/10.1016/j.jastp.2017.02.001

Ballinger, A. P., Chilson, P. B., Palmer, R. D., & Mitchell, N. J. (2008). On the validity of the ambipolar diffusion assumption in the polar mesopause region. *Annales de Geophysique*, *26*, 3439–3443. https://doi.org/10.5194/angeo-26-3439-2008

Batista, P. P., Clemesha, B. R., Tokumoto, A. S., & Lima, L. M. (2004). Structure of the mean winds and tides in the meteor region over Cachoeira Paulista, Brazil (22.7°S, 45°W) and its comparison with models. *Journal of Atmospheric and Solar - Terrestrial Physics*, *66*, 623–636. https://doi.org/10.1016/j.jastp.2004.01.014

Buriti, R. A., Takahashi, H., & Gobbi, D. (2001). First results from mesospheric airglow observations at 7.5°S. *Revista Brasileira de Geografia*, *19*, 169–176. https://doi.org/10.1590/S0102-261X2001000200005

Chilson, P. B., Czechowsky, P., & Schmidt, G. (1996). A comparison of ambipolar diffusion coefficients in meteor trains using VHF radar and UV lidar. *Geophysical Research Letters*, *23*, 2745–2748. https://doi.org/10.1029/96GL02577

deWit, R. J., Hibbins, R. E., Espy, P. J., & Mitchell, N. J. (2013). Interannual variability of mesopause zonal winds over Ascension Island: Coupling to the stratospheric QBO. *Journal of Geophysical Research: Space Physics*, *118*, 12,052–12,060. https://doi.org/10.1002/2013JD020203

Dunkerton, T. J. (1982). Theory of the mesopause semiannual oscillation. *Journal of the Atmospheric Sciences*, *39*, 2681. https://doi.org/10.1175/1520-0469(1982)039<2681:TOTMSO>2.0.CO;2

Dyrland, M. E., Hall, C. M., Mulligan, F. J., Tsutsumi, M., & Sigernes, F. (2010). Improved estimates for neutral air temperatures at 90 km and 78°N using satellite and meteor radar data. *Radio Science*, *45*, RS4006. https://doi.org/10.1029/2009RS004344

Garcia, R. R., Dunkerton, T. J., Lieberman, R. S., & Vincent, R. A. (1997). Climatology of the semiannual oscillation of the tropical middle atmosphere. *Journal of Geophysical Research*, *102*(D22), 26,019–26,032. https://doi.org/10.1029/97JD00207

Gattinger, R. L., Kyrölä, E., Boone, C. D., Evans, W. F. J., Walker, K. A., McDade, I. C., et al. (2013). The roles of vertical advection and eddy diffusion in the equatorial mesospheric semi-annual oscillation (MSAO). *Atmospheric Chemistry and Physics*, *13*, 7813–7824. https://doi.org/10.5194/acp-13-7813-2013

Hall, C. M., Aso, T., Tsutsumi, M., Höffner, J., Sigernes, F., & Holdsworth, D. A. (2006). Neutral air temperatures at 90 km and 70°N and 78°N. *Journal of Geophysical Research*, *111*, D14105. https://doi.org/10.1029/2005JD006794

Hall, C. M., Aso, T., Tsutsumi, M., Nozawa, S., Manson, A. H., & Meek, C. E. (2005). Letter to the editor testing the hypothesis of the influence of neutral turbulence on the deduction of ambipolar diffusivities from meteor trail expansion. *Annales de Geophysique*, *23*, 1071–1073. https://doi.org/10.5194/angeo-23-1071-2005

Hall, C. M., Dyrland, M. E., Tsutsumi, M., & Mulligan, F. J. (2012). Temperature trends at 90 km over Svalbard, Norway (78°N, 16°E), seen in one decade of meteor radar observations. *Journal of Geophysical Research*, *117*, D08104. https://doi.org/10.1029/2011JD017028

Hocking, W. K. (1999). Temperatures using radar-meteor decay times. *Geophysical Research Letters*, *26*, 3297–3300. https://doi.org/10.1029/1999GL003618

Hocking, W. K., Singer, W., Bremer, J., Mitchell, N. J., Batista, P., Clemesha, B., et al. (2004). Meteor radar temperatures at multiple sites derived with SKiYMET radars and compared to OH, rocket and lidar measurements. *Journal of Atmospheric and Solar - Terrestrial Physics*, *66*, 585–593. https://doi.org/10.1016/j.jastp.2004.01.011

Hocking, W. K., Thayaparan, T., & Jones, J. (1997). Meteor decay times and their use in determining a diagnostic mesospheric temperature-pressure parameter: Methodology and one year of data. *Geophysical Research Letters*, *24*, 2977–2980. https://doi.org/10.1029/97GL03048

Holdsworth, D. A., Morris, R. J., Murphy, D. J., Reid, I. M., Burns, G. B., & French, W. J. R. (2006). Antarctic mesospheric temperature estimation using the Davis mesosphere-stratosphere-troposphere radar. *Journal of Geophysical Research*, *111*, D05108. https://doi.org/10.1029/2005JD006589

Huang, F. T., Mayr, H. G., Reber, C. A., Russell, J. M., Mlynczak, M. G., & Mengel, J. G. (2006). Stratospheric and mesospheric temperature variations for the quasi-biennial and semiannual (QBO and SAO) oscillations based on measurements from SABER (TIMED) and MLS (UARS). *Annales de Geophysique*, *24*, 3719–3730. https://doi.org/10.5194/angeo-24-2131-2006

Huang, F. T., Mayr, H. G., Russell, J. M., & Mlynczak, M. G (2016). Ozone and temperature decadal responses to solar variability in the mesosphere and lower thermosphere, based on measurements from SABER on TIMED. *Annales de Geophysique*, *34*, 29–40. https://doi.org/10.5194/angeo-34-29-2016

Jones, J., Webster, A. R., & Hocking, W. K. (1998). An improved interferometer design for use with meteor radars. *Radio Science*, *33*(1), 55–65. https://doi.org/10.1029/97RS03050

Kumar, K. K. (2007). Temperature profiles in the MLT region using radar-meteor trail decay times: Comparison with TIMED/SABER observations. *Geophysical Research Letters*, *34*, L16811. https://doi.org/10.1029/2007GL030704

Lee, C., Kim, J.-H., Jee, G., Lee, W., Song, I.-S., & Kim, Y. H. (2016). New method of estimating temperatures near the mesopause region using meteor radar observations. *Geophysical Research Letters*, *43*, 10,580–10,585. https://doi.org/10.1002/2016GL071082

Lima, L. M., Alves, E. O., Batista, P. P., Clemesha, B. R., Medeiros, A. F., & Buriti, R. A. (2012). Sudden stratospheric warming effects on the mesospheric tides and 2-day wave dynamics at 7°S. *Journal of Atmospheric and Solar - Terrestrial Physics*, *78*, 99–107. https://doi.org/10.1016/j.jastp.2011.02.013

Lima, L. M., Araujo, L. R., Alves, E. O., Batista, P. P., & Clemesha, B. R. (2015). Variations in meteor heights at 22.7°S during solar cycle 23. *Journal of Atmospheric and Solar - Terrestrial Physics*, *133*, 139–144. https://doi.org/10.1016/j.jastp.2015.08.015

Lima, L. M., Paulino, A. R., Medeiros, A. F., Buriti, R. A., Batista, P. P., Clemesha, B. R., et al. (2007). First observation of the diurnal and semidiurnal oscillation in the mesospheric winds over São João do Cariri-PB, Brazil. *Revista Brasileira de Geofísica*, *25*, 35–41. https://doi.org/10.1590/S0102-261X2007000600005

Liu, L., Liu, H., Le, H., Chen, Y., Sun, Y.-Y., Ning, B., et al. (2017). Mesospheric temperatures estimated from the meteor radar observations at Mohe China. *Journal of Geophysical Research: Space Physics*, *122*, 2249–2259. https://doi.org/10.1002/2016JA023776

McKinley, D. W. R. (1961). *Meteor Science and Engineering*. New York: McGraw-Hill.

Meek, C. E., Manson, A., Hocking, W. K., & Drummond, J. R. (2013). Eureka, 80° N, SKiYMET meteor radar temperatures compared with Aura MLS values. *Annales de Geophysique*, *31*, 1267–1277. https://doi.org/10.5194/angeo-31-1267-2013

Offermann, D., Hoffmann, P., Knieling, P., Koppmann, R., Oberheide, J., & Steinbrecht, W. (2010). Long-term trends and solar cycle variations of mesospheric temperatures and dynamics. *Journal of Geophysical Research*, *115*, D18127. https://doi.org/10.1029/2009JD013363

Peña-Ortiz, C., Schmidt, H., Giorgetta, M. A., & Keller, M. (2010). QBO modulation of the semiannual oscillation in MAECHAM5 and HAMMONIA. *Journal of Geophysical Research*, *115*, D21106. https://doi.org/10.1029/2010JD013898

Picone, J. M., Hedin, A. E., Drob, D. P., & Aikin, A. C. (2002). NRLMSISE-00 empirical model of the atmosphere: Statistical comparisons and scientific issues. *Journal of Geophysical Research*, *107*(A12), 1468. https://doi.org/10.1029/2002JA009430

Remsberg, E. E., Marshall, B. T., Garcia-Comas, M., Krueger, D., Lingenfelser, G. S., Martin-Torres, J., et al. (2008). Assessment of the quality of the version 1.07 temperature-versus-pressure profiles of the middle atmosphere from TIMED/SABER. *Journal of Geophysical Research*, *113*, D17101. https://doi.org/10.1029/2008JD010013

Roble, R. G., & Dickinson, R. E. (1989). How will changes in carbon dioxide and methane modify the mean structure of the mesosphere and thermosphere? *Geophysical Research Letters*, *46*(12), 1441–1444. https://doi.org/10.1029/GL016i012p01441

Sassi, F., & Garcia, R. R. (1997). The role of equatorial waves forced by convection in the tropical semiannual oscillation. *Journal of the Atmospheric Sciences*, *54*, 1925–1942. https://doi.org/10.1175/1520-0469(1997)054<1925:TROEWF>2.0.CO;2

Scargle, J. D. (1982). Studies in astronomical time series analysis. II. Statistical aspects of spectral analysis of unevenly spaced data. *The Astrophysical Journal*, *263*, 835–853. https://doi.org/10.1086/160554

She, C.-Y., Krueger, D. A., & Yuan, T (2015). Long-term midlatitude mesopause region temperature trend deduced from quarter century (1990–2014) Na lidar observations. *Annales de Geophysique*, *33*, 363–369. https://doi.org/10.5194/angeo-33-363-2015

Shepherd, M. G., Evans, W. F. J., Hernandez, G., Offermann, D., & Takahashi, H. (2004). Global variability of mesospheric temperature: Mean temperature field. *Journal of Geophysical Research*, *109*, D24117. https://doi.org/10.1029/2004JD005054

Takahashi, H., Clemesha, B. R., & Batista, P. P. (1995). Predominant semi-annual oscillation of the upper mesospheric airglow intensities and temperatures in the equatorial region. *Journal of Atmospheric and Solar - Terrestrial Physics*, *57*, 407–414. https://doi.org/10.1016/0021-9169(94)E0006-9

Takahashi, H., Nakamura, T., Shiokawa, K., Tsuda, T., Lima, L. M., & Gobbi, D. (2004). Atmospheric density and pressure inferred from the meteor diffusion coefficient and airglow O_2b temperature in the MLT region. *Earth, Planets and Space*, *56*, 249–258. https://doi.org/10.1186/BF03353407

Takahashi, H., Wrasse, C. M., Gobbi, D., Nakamura, T., Shiokawa, K., & Lima, L. M. (2005). Airglow OH emission height inferred from the OH temperature and meteor trail diffusion coefficient. *Advances in Space Research*, *35*, 1940–1944. https://doi.org/10.1016/j.asr.2005.05.052

Venturini, M. S., Bageston, J. V., Caetano, N. R., Peres, L. V., Bencherif, H., & Schuch, N. J. (2018). Mesopause region temperature variability and its trend in southern Brazil. *Annales de Geophysique*, *36*, 301–310. https://doi.org/10.5194/angeo-36-301-2018

Yi, W., Xue, X., Chen, J., Dou, X., Chen, T., & Li, N. (2016). Estimation of mesopause temperatures at low latitudes using the Kunming meteor radar. *Radio Science*, *51*, 130–141. https://doi.org/10.1002/2015RS005722

Younger, J. P., Lee, C. S., Reid, I. M., Vincent, R. A., Kim, Y. H., & Murphy, D. J. (2014). The effects of deionization processes on meteor radar diffusion coefficients below 90 km. *Journal of Geophysical Research: Atmospheres*, *119*, 10,027–10,043. https://doi.org/10.1002/2014JD021787